PAPER

Check for updates

Development of prediction model for cloud point of thermo-responsive polymers by experiment-oriented materials informatics†

Mai Hayakawa,[a] Kosuke Sakano,[a] Rei Kumada,[a] Haruka Tobita,[a] Yasuhiko Igarashi,[b] Daniel Citterio, [ID] [a] Yuya Oaki [ID] [a] and Yuki Hiruta [ID] *[a]

Thermo-responsive polymers having a lower critical solution temperature (LCST) have attracted attention for biological applications such as drug delivery, diagnosis, and coating materials. In recent years, research on predicting LCST by utilizing machine learning has been conducted. However, since these methods targeted only copolymers combining specific monomer structures, they are not versatile, and multiple trials are still required to obtain new thermo-responsive polymers with the desired LCST. In this study, a prediction model for cloud point temperature (T_{CP}) was built by a combination of materials informatics and chemical insight, named sparse modeling for small data (SpM-S) using a small dataset of polymers collected from the literature as training data. This approach created a model that is interpretable, easy to calculate, and versatile. The prediction accuracy was validated using data from different literature sources and experimental test data. The model was able to predict the T_{CP} of polymers containing monomers not included in the dataset as well as polymers containing monomers included in the dataset. The predictive model has the potential to guide the design of new thermo-responsive polymers, and to contribute to efficient development of thermo-responsive polymers.

Introduction

Stimuli-responsive polymers, which change their properties in response to specific external stimuli, such as temperature,[1] light,[2] pH,[3] and ions,[4] are used in a wide range of fields, such as drug delivery systems, diagnostics, and coating materials.[5–8]

Among them, thermo-responsive polymers, which exhibit a temperature-dependent phase transition, are one of the most widely studied stimuli-responsive polymers. Thermo-responsive polymers have a lower critical solution temperature (LCST) or upper critical solution temperature (UCST) in aqueous solution.[9] Compared to UCST-type polymers, many studies have been reported on LCST-type polymers applied to the biomedical field, because they undergo a phase transition at physiological temperature and conditions,[10] which are less sensitive to pH and ionic strength.[11–13] Thanks to these advantages, LCST-type polymers have been actively studied.[12,14] Experimental characterization of such LCST phenomena has been studied using various measurement methods, including cloud point measurements,[15] dynamic light scattering,[16] and differential scanning calorimetry.[17] Among them, simple assays of clouding behaviour are still the most common to study this type of phase separation process, which is important in various applications of thermo-responsive polymers.[18]

In designing thermo-responsive polymers, the control of LCST is an important issue for applications. The LCSTs of thermo-responsive polymers can be controlled by changing monomer ratio,[19–22] molecular weight,[23,24] and the structure of end groups.[25,26] Furthermore, phase transition properties of thermo-responsive polymers are affected by the concentrations of ionic species,[27,28] and the content of organic solvents.[29,30] In addition to these experimental methods, some studies have predicted cloud point temperature (T_{CP}) by creating regression equations based on molecular weight, degree of polymerization, or monomer ratio.[31–33] To develop new thermo-responsive polymers, it is necessary to appropriately select type and composition ratio of monomers from an unlimited number of possible combinations. Therefore, controlling LCST of thermo-responsive polymers remains a challenge for researchers.

Recently, machine learning has been applied to predict and control the physical properties of materials and explore new ones.[34–37] Although applying machine learning to polymers is generally difficult due to the complex structure–function relationships,[38] it is beginning to be used in the field of thermo-responsive polymers.[39,40] Kumar and co-workers showed the prediction and control of the T_{CP} of poly(2-oxazo-

[a]*Department of Applied Chemistry, Faculty of Science and Technology, Keio University, 3-14-1 Hiyoshi, Kohoku-ku, Yokohama 223-8522, Japan. E-mail: hiruta@applc.keio.ac.jp*
[b]*Faculty of Engineering, Information and Systems, University of Tsukuba, 1-1-1 Tennodai, Tsukuba 305-8573, Japan*

line) *via* machine learning.[39] The method of gradient boosting with decision trees enabled highly accurate T_{CP} control in a design space consisting of four repeating units and various molecular weights. Although the model was limited to the prediction of these structures because of the descriptors such as molecular weight and degree of polymerization of the copolymers in the four poly(2-oxazoline) repeating units, they provide motivation to extend the study of T_{CP} control using machine learning. In addition, other groups have reported the prediction of T_{CP} of polymers consisting of *N*-isopropylacrylamide (NIPAAm) and methoxy triethyleneglycol acrylate (MTGA) in aqueous salt solutions, utilizing a technique called support vector regression.[40] Although the application of this model is limited to poly(NIPAAm-MTGA), it shows that machine learning can be used to understand the phase-transition behaviour of LCST-type thermo-responsive polymers. However, these prediction models were applicable only to copolymers of specific monomer combinations. They cannot be applied to the prediction of thermo-responsive polymers with monomers or copolymer compositions not used in the models. In addition, these studies have fixed explanatory variables and have not reached the point of searching for variables that contribute significantly to T_{CP} among many chemical parameters. There is still room for improvement in T_{CP} prediction model development. Therefore, we have attempted to establish guidelines for the T_{CP} of thermo-responsive polymers using a new approach based on a machine learning method for small data.

In general, the success of prediction or exploration for materials depends on the amount of data.[36] However, sufficient data is not always available for the target materials. Our group has focused on sparse modeling for small data (SpM-S). Sparse modeling is an approach to represent the whole of high-dimensional data using a limited number of descriptors extracted by machine learning.[41] This approach has been applied to a variety of fields, such as image data and image compressions.[42] It is applicable to small data because of extraction of a limited number of significant descriptors from high-dimensional data.[43] SpM-S, which combines sparse modeling and chemical insights, has been successfully used to predict nanosheet size and yield in an example of process optimization and to explore new organic anode and cathode materials for lithium ion batteries in materials exploration.[43–45] Here, we applied SpM-S to develop an T_{CP} prediction model for thermo-responsive polymers based on a small dataset collected from the literature. Furthermore, the model was validated with the T_{CP} prediction of thermo-responsive polymers with monomers and copolymer compositions that were not incorporated in the training dataset (Fig. 1).

Experimental

Data collection of objective variables *y* from the literature

Objective variables for training data, T_{CP}s of the polymers (the temperature at 50% of the optical transmittance of the polymer solution), were collected from 6 references.[46–51]

Fig. 1 Overview of this work: (a) 12 potential factors for T_{CP} as explanatory variables. (b) Objective variables for training data of non-brushy polymers from 5 literature references. (c) Preparation of small dataset consisting of training data and explanatory variables. (d) SpM-S combining machine learning and chemical insight. (e) Validation of prediction model with test data.

Data collection and calculation for explanatory variables

$x_{1–3}$ were collected from 6 references.[46–51] The molecular weights, and poly dispersity index (PDI) of the polymers ($x_{1–2}$) were collected from gel permeation chromatography (GPC) analysis. Concentrations of polymers (x_3) were collected from experimental values of optical transmittance measurements. Hansen-solubility parameters ($x_{4–6}$) were calculated by the HSP software (HSPiP 5th edition ver. 5.3.06). Chemical properties of monomers ($x_{7–12}$) were calculated by ChemDraw (ver. 21.0.0).

The dataset containing 28 *y* and x_n ($n = 1–12$) was prepared (Table S1 in the ESI†). Exhaustive search with linear regression (ES-LiR) was performed by Python. The results were summarized in the weight diagram to extract the descriptors by combination with our chemical insights. The linear prediction model was prepared by the selected descriptors after five-fold cross validation.

Chemicals

N-Isopropylacrylamide (NIPAAm), kindly provided by KJ Chemicals Co., Ltd (Tokyo, Japan), was purified by recrystallization from *n*-hexane, and then dried under vacuum. 2,2′-Azobisisobutyronitrile (AIBN), 2-(dodecylthiocarbonothioylthio)-2-methylpropionic acid (DDMAT), *N*,*N*-dimethylacrylamide (DMAAm) and 1,3,5-trioxane were purchased from Tokyo Chemical Industries (Tokyo, Japan). DMAAm was purified by passing through a short column of activated basic alumina to remove the inhibitor. *n*-Propylamine was purchased from Nakalai Tesque (Kyoto, Japan). Acryloyl chloride was purchased from Sigma-Aldrich (St Louis, MO, USA). *N*-*n*-Propylacrylamide (NNPAAm) was synthesized with *n*-propylamine and acryloyl chloride as previously reported.[52] Ultrapure

water (18.2 MΩ cm) was obtained from a PURELAB flex water purification system (ELGA, Veolia Water, Marlow, U.K.).

General procedure for the synthesis of thermo-responsive polymers

Thermo-responsive polymers were synthesized by reversible addition–fragmentation chain transfer (RAFT) polymerization. The corresponding monomers, DDMAT as RAFT chain transfer agent (CTA), AIBN as radical initiator, and the internal standard of 1,3,5-trioxane (10 eq. to DDMAT) were dissolved in 1,4-dioxane. The reaction mixture was degassed by bubbling with N_2 for 30 min, and heated at 70 °C for 17 h. The reaction mixtures were purified by reprecipitation in diethyl ether, followed by drying to a white powder.

P(NIPAAm$_{90}$-co-DMAAm$_{10}$). NIPAAm (1.37 g, 12.1 mmol, 320 eq.), DMAAm (0.133 g, 1.34 mmol, 36 eq.), AIBN (3.1 mg, 0.019 mmol, 0.5 eq.), DDMAT (13.6 mg, 0.0373 mmol, 1.0 eq.), and 1,4-dioxane (3 mL) were used as reaction mixture. NIPAAm, and DMAAm conversion rates were 100%, and 100%, respectively.

P(NIPAAm$_{70}$-co-DMAAm$_{30}$). NIPAAm (1.09 g, 9.64 mmol, 260 eq.), DMAAm (0.409 g, 4.12 mmol, 110 eq.), AIBN (3.1 mg, 0.019 mmol, 0.5 eq.), DDMAT (13.7 mg, 0.0376 mmol, 1.0 eq.), and 1,4-dioxane (3 mL) were used as reaction mixture. NIPAAm, and DMAAm conversion rates were 100%, and 100%, respectively.

P(NIPAAm$_{50}$-co-DMAAm$_{50}$). NIPAAm (1.33 g, 11.8 mmol, 190 eq.), DMAAm (1.17 g, 11.8 mmol, 190 eq.), AIBN (4.9 mg, 0.031 mmol, 0.5 eq.), DDMAT (22.5 mg, 0.0617 mmol, 1.0 eq.), and 1,4-dioxane (5 mL) were used as reaction mixture. NIPAAm, and DMAAm conversion rates were 100%, and 100%, respectively.

P(NIPAAm$_{90}$-co-NNPAAm$_{10}$). NIPAAm (0.900 g, 9.08 mmol, 360 eq.), NNPAAm (0.0996 g, 0.880 mmol, 35 eq.), AIBN (2.1 mg, 0.013 mmol, 0.5 eq.), DDMAT (9.1 mg, 0.025 mmol, 1.0 eq.), and 1,4-dioxane (2 mL) were used as reaction mixture. NIPAAm, and NNPAAm conversion rates were 100%, and 100%, respectively.

P(NIPAAm$_{70}$-co-NNPAAm$_{30}$). NIPAAm (0.700 g, 6.18 mmol, 250 eq.), NNPAAm (0.300 g, 2.65 mmol, 110 eq.), AIBN (2.1 mg, 0.013 mmol, 0.5 eq.), DDMAT (9.1 mg, 0.025 mmol, 1.0 eq.), and 1,4-dioxane (2 mL) were used as reaction mixture. NIPAAm, and NNPAAm conversion rates were 100%, and 100%, respectively.

P(NIPAAm$_{50}$-co-NNPAAm$_{50}$). NIPAAm (0.500 g, 4.42 mmol, 180 eq.), NNPAAm (0.500 g, 4.42 mmol, 180 eq.), AIBN (2.1 mg, 0.013 mmol, 0.5 eq.), DDMAT (9.1 mg, 0.025 mmol, 1.0 eq.), and 1,4-dioxane (2 mL) were used as reaction mixture. NIPAAm, and NNPAAm conversion rates were 100%, and 100%, respectively.

Characterization of thermo-responsive polymers

^{1}H NMR spectra were recorded on a JNM ECA-500 spectrometer (JEOL, Japan). All chemical shifts are relative to an internal standard of non-deuterated solvent residual peaks (CDCl$_3$: δ = 7.26 ppm or CD$_3$OD δ = 3.31 ppm). The molecular weights of polymers ($M_{n,NMR}$) are calculated using starting monomers to RAFT CTA ratios and the monomer conversion

of each reaction monitored by ^{1}H NMR. The molecular weights ($M_{n,GPC}$) and PDIs of the polymers were determined by a GPC system (Prominence, CMB-20A system controller, DGU-20A3R degasser, LC-20AR pump, SIL-20ACHT autosampler, RID-20A refractive index detector, and CTO-20AC column oven; Shimadzu, Kyoto, Japan), and using columns: TSKgel guardcolumnα, two TSKgelα-M (TOSOH, Tosoh, Japan) connected in series; mobile phase: DMF containing 10 mM LiBr used as eluent at a flow rate of 0.7 mL min^{-1} at 40 °C. Calibrations were done with polyethylene oxide standards. The T_{CP}s of the polymers were determined by measuring their optical transmittance in aqueous solution (0.5 w/v%). The optical transmittance was measured at various temperatures at 600 nm using a UV-Vis spectrophotometer (V-730BIO, JASCO, Tokyo, Japan). The temperature was controlled using an ETCS-761 Peltier system (JASCO) and a CTU-100 circulating thermostat unit (JASCO) at a heating rate of 0.1 °C min^{-1}. The T_{CP}s were determined as the temperature at 50% of the optical transmittance of the polymer solution.

Results and discussion

Selection of literature references and explanatory variables for the dataset

Since LCST is defined by several measurement methods, such as optical transmittance, dynamic light scattering, and differential scanning calorimetry, LCSTs, which represent the objective variable in this work, were collected only from references in which it is defined as the temperature at 50% of optical transmittance.

First, T_{CP} was set as the objective variable, and factors that could be related to it were collected as explanatory variables. The explanatory variables (x_n: n = 1–12) were selected and prepared based on our insights and experience (Fig. 1a, Table 1 and Table S1†). They included both parameters related to polymers (x_n: n = 1–3) and those related to monomers (x_n: n = 4–12). Molecular weight and PDI as typically measured when polymers are synthesized were selected as explanatory variables for the polymers. As an experimental value when measuring T_{CP}, the polymer concentration is also selected as explanatory variable. Physicochemical parameters that can be easily calculated by HSPiP and ChemDraw were selected as explanatory variables for the monomers used in polymers. This allows us to build an interpretable and simple predictive model for T_{CP} without experiments and complex simulation and calculation. In the case of copolymers, the parameters of each monomer were averaged by composition ratio and then used as explanatory variables. It is not necessary to separate the case for homopolymers and copolymers. In addition, it allows us to apply to copolymers constructed of more than 3 monomers. In this study, the influence of terminal substituent characteristics on T_{CP} was considered to be low, and it was decided not to include it as an explanatory variable.

Previously, it has been reported that the dominant parameter determining T_{CP} is different between copolymers con-

Table 1 The list of explanatory variables

Polymers		Monomers	
x_n	Parameters	x_n	Parameters
1	Molecular weight[a]	4	HSP dispersity[b]
2	Poly dispersity (PDI)[a]	5	HSP polarity[b]
3	Concentration[a]	6	HSP hydrogen bonding[b]
		7	Molecular weight
		8	Boiling point[c]
		9	Molar refractive index[c]
		10	Topological polar surface area[c]
		11	C log P^c
		12	CMR[c]

[a] Literature data. [b] Calculated data by HSPiP. [c] Calculated data by ChemDraw.

Scheme 1 The structures of monomers included in the dataset.

taining monomers of a brushy nature such as oligo(ethylene glycol) methacrylate (OEGMA) and those containing only non-brushy monomers. As for brush copolymers, graft density had great influence on the T_{CP}, whereas for non-brush copolymers, surface area-normalized hydrophobicity of copolymers has strong influence on the T_{CP}. Considering this knowledge, our predictive model, which uses the average value from the composition ratio of each monomer as explanatory variables, is appropriate for limited application to T_{CP} prediction for non-brushy copolymers. In the present work, reported T_{CP} data of non-brushy polymers, which consisted of monomers 1 to 15, were manually collected from literature references (Fig. 1b, Scheme 1, Fig. S1 and Tables S1, S2†).[46–50] This dataset covers a variety of homopolymers and random copolymers, not limited to any particular structure. Finally, a small training dataset containing 28 objective variables (y) and 12 explanatory variables (x) was prepared (Fig. 1c and Table S1†).

Construction of the prediction model

ES-LiR was used to extract the descriptors. In ES-LiR, linear regression models are prepared by all possible combinations of x_n, $2^n - 1$ combinations. In this case, a total of $2^{12} - 1(4094)$ regression models were prepared, and the results were sorted in ascending order of the cross-validation error (CVE).

The weight diagram shows the top 1000 prediction models with the lowest CVE values (Fig. 1d and 2). In the weight diagram, the coefficients of the models were indicated by a cold color for negative correlations and a warm color for positive correlations. Interpretation of the weight diagram and construction of the final model were performed from a chemical perspective. In the present results, x_3 (concentration of polymer), x_5 (HSP-polarity of monomer), x_{10} (tPSA of monomer), and x_{11} (C log P of monomer) were densely blue colored in the weight diagram. From these variables, we selected the final descriptors, x_3 (concentration of polymer), x_5 (HSP-polarity of monomer), x_{11} (C log P of monomer) based on chemical insights. First, it is known that polymer chains tend to aggregate in aqueous solution at higher polymer concentrations. Therefore, it was reasonable that the explanatory variable x_3 (concentration of polymer) was extracted as negatively

Fig. 2 Weight diagram of ES-LiR analysis representing the top 1000 prediction model with the lowest CVE values by color. The warm, cool and non-color show positive, negative and zero coefficients, respectively.

correlated descriptor. Next, x_5 (HSP-polarity of monomer) was extracted because it is one of the parameters related to solubility. In addition, x_{11} (C log P of monomer) was extracted. C log P is the calculated value of the distribution equilibrium between octanol and water, which is the hydrophobicity index. The smaller the value, the more hydrophilic the compound. With increasing hydrophilicity, T_{CP} also increases. Therefore, it is considered as a negatively correlated parameter. In contrast, x_{10} (tPSA of monomer) was not included in the final predictive model even though it was extracted as a negatively correlated descriptor. From the chemical perspective, an increase in polar surface area is expected not to decrease, but to increase the T_{CP} due to overall increase of polarity. Therefore, tPSA was removed from the final model based on chemical insights. Surprisingly, x_1 (molecular weight of polymer) positively correlated to cloud-point, while it should correlate negatively.[53] This is probably because the molecular weights of polymers are determined by GPC, and thus no correlation in absolute molecular weight could be obtained among the literature references due to the differences in the GPC columns used and types of standard polymer samples. Based on the above considerations, the prediction model was described using x_3

(Concentration of polymer), x_5 (HSP-polarity of monomer) and x_{11} (C log P of monomer) (Fig. 1d and eqn (1)) with a root mean squared error (RMSE) of 7.13 °C, where x_n are normalized by the frequency distribution such that the mean is 0 and the standard deviation is 1.

$$y = -0.520x_3 - 25.8x_5 - 21.4x_{11} + 35.3 \quad (1)$$

Synthesis of thermo-responsive copolymers for validation

To evaluate the validity of the constructed prediction model, thermo-responsive copolymers with non-brushy monomers

Fig. 3 The structure of synthesized copolymers for use as test data.

were synthesized. One of the monomers used to synthesize copolymers was *N*-isopropylacrylamide (NIPAAm), and its homopolymer, poly(*N*-isopropylacrylamide) (PNIPAAm) is the most well-known thermo-responsive polymer. NIPAAm was copolymerized with *N,N*-dimethylacrylamide (DMAAm) or *N*-propylacrylamide (NNPAAm), which were selected to have higher or lower T_{CP} than PNIPAAm (Fig. 3). Six types of copolymers with different NIPAAm/DMAAm or NIPAAm/NNPAAm ratios were synthesized by RAFT polymerization. The composition ratio of NIPAAm was set to be identical in each polymer, ranging from 50% to 90%.

Molecular weight was measured using GPC (Fig. S2†), and narrow PDI of synthesized copolymers was confirmed. Optical transmittance measurements were then performed using a UV-vis spectrophotometer to obtain cloud-point test data. The temperature-dependent optical transmittances of synthesized thermo-responsive polymers in water are shown in Fig. 4. All polymers exhibited a sharp phase-transition at different temperatures according to the monomer composition ratio. The T_{CP} of copolymers depended on the composition ratio (Table 2). In the case of P(NIPAAm-*co*-DMAAm), a lower content of NIPAAm resulted in an increase in T_{CP}, while the opposite trend was
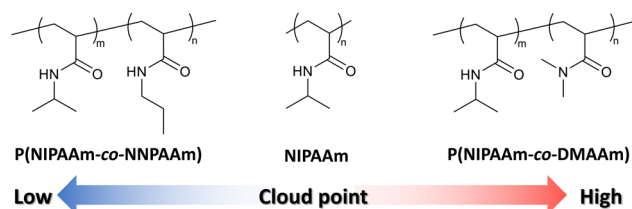

Fig. 4 Thermo-responsiveness of synthesized polymers for test data: (a) Optical transmittance as a function of temperature for P(NIPAAm-*co*-DMAAm) aqueous solution, and (b) P(NIPAAm-*co*-NNPAAm) aqueous solution (0.5 w/v%). (c) The values of T_{CP} of P(NIPAAm-*co*-DMAAm) and P(NIPAAm-*co*-NNPAAm) as a function of composition ratios of NIPAAm.

Table 2 Physicochemical properties of PNIPAAm-based thermo-responsive copolymers

Polymer	Composition ratios of NIPAAm in feed [mol%]	Actual composition ratios of NIPAAm [mol%]	$M_{n,NMR}$	$M_{n,GPC}$	PDI	T_{CP}[°C]
P(NIPAAm$_{90}$-*co*-DMAAm$_{10}$)	90	90	40 600	25 800	1.20	35.4
P(NIPAAm$_{70}$-*co*-DMAAm$_{30}$)	70	70	39 700	25 600	1.16	44.7
P(NIPAAm$_{50}$-*co*-DMAAm$_{50}$)	50	50	40 900	21 600	1.27	64.0
P(NIPAAm$_{90}$-*co*-NNPAAm$_{10}$)	90	90	40 400	28 800	1.18	31.7
P(NIPAAm$_{70}$-*co*-NNPAAm$_{30}$)	70	70	40 300	26 600	1.23	29.2
P(NIPAAm$_{50}$-*co*-NNPAAm$_{50}$)	50	50	40 400	28 300	1.27	27.1

observed for P(NIPAAm-*co*-NNPAAm). In summary, test data for the prediction model was obtained over a wide temperature range by synthesizing NIPAAm-based thermo-responsive copolymers.

Validation of prediction model with literature data and synthesized polymers

The constructed prediction model was validated using the test data from references that have not been included in the model building dataset,[49,54] and synthesized polymers, as described above (Fig. 1e and Tables S3–S5†). Test data from a literature reference and the experiment was substituted into the prediction model (eqn (1)). The higher the T_{CP}, the greater the deviation between the measured and the estimated data, predicting a lower T_{CP} than the measured data (Fig. 5a). To improve prediction accuracy of the T_{CP} in the higher temperature range, the coefficients of the prediction model (eqn (1)) were corrected using a literature reference providing data for higher T_{CP}[51] (Fig. S3 and Tables S6, S7†). The final prediction model was constructed following equation (eqn (2)) with an RMSE of 8.88 °C.

$$y = -1.00x_3 - 33.0x_5 - 34.3x_{11} + 37.4 \qquad (2)$$

The RMSE was 5.43 °C for the test data from literature references (Fig. 5b, green plots). This value was comparable to the training data, indicating high prediction accuracy. Prediction accuracy was also confirmed with the synthesized copolymers, P(NIPAAm-*co*-DMAAm) whose monomer species were used in the dataset. The test data of P(NIPAAm-*co*-DMAAm), whose T_{CP} exhibits a higher value than that of PNIPAAm, had an RMSE of 7.79 °C (Fig. 5b, orange plots). This RMSE value was also comparable to the training data, indicating high prediction accuracy. NIPAAm and DMAAm are the monomer species included in the dataset, respectively, but not their copolymers. This result indicates that this model can be applied to T_{CP} prediction of polymers whose monomer combination is not included in the dataset. The applicability of this model was also investigated for copolymers containing a monomer not included in the dataset. P(NIPAAm-*co*-NNPAAm), which exhibits a lower

T_{CP} than PNIPAAm, had an RMSE of 1.87 °C, showing high prediction accuracy (Fig. 5b, yellow plot). As for monomers used to construct the polymer, NIPAAm has been included in the dataset, while NNPAAm was not. Considering this result, this prediction model was also able to predict T_{CP} for polymers composed of monomers not in the dataset.

Conclusions

The T_{CP} prediction of thermo-responsive polymers was achieved with the assistance of materials informatics with SpM-S. The descriptors, concentration of polymer, HSP-polarity of monomer, and C log P of monomer, were extracted by the combination of ES-LiR and chemical insights. Finally, the regression equation for T_{CP} prediction was obtained from 33 datasets. To validate the constructed prediction model, six types of copolymers with different NIPAAm/DMAAm or NIPAAm/NNPAAm ratios were synthesized. The constructed model showed good correlation with the experimentally measured the T_{CP}s of P(NIPAAm-*co*-DMAAm) and P(NIPAAm-*co*-NNPAAm) and the T_{CP}s extracted from literature references over a wide temperature range from 20 °C to 65 °C. To the best of our knowledge, this prediction model for T_{CP} is the first example applied to predict polymers with monomers and combinations not included in the dataset. In addition, the model has the advantage of being interpretable, simple to calculate, and versatile, and the potential to provide a rough guideline to T_{CP} for thermo-responsive polymers. This study is expected to lead to the efficient development of LCST-type polymers.

Author contributions

Mai Hayakawa: methodology, investigation, writing – original draft. Kosuke Sakano: formal analysis. Rei Kumada: writing – review & editing. Haruka Tobita: formal analysis. Yasuhiko Igarashi: software, supervision. Daniel Citterio: writing – review & editing, supervision. Yuya Oaki: conceptualization, writing – review & editing, supervision. Yuki Hiruta: conceptualization, methodology, writing – review & editing, supervision, project administration, funding acquisition.

Conflicts of interest

There are no conflicts to declare.

Acknowledgements

Fig. 5 The relationship between estimated T_{CP}s from prediction model and measured values: (a) Compared by prediction model of eqn (1). (b) Compared by prediction model of eqn (2) with corrected coefficients.

References

1 K. Suwa, K. Morishita, A. Kishida and M. Akashi, *J. Polym. Sci., Part A: Polym. Chem.*, 1997, **35**, 3087–3094.

2 F. D. Jochum and P. Theato, *Chem. Soc. Rev.*, 2013, **42**, 7468–7483.

3 S. Dai, P. Ravi and K. C. Tam, *Soft Matter*, 2008, **4**, 435.

4 X.-J. Ju, L. Liu, R. Xie, C. H. Niu and L.-Y. Chu, *Polymer*, 2009, **50**, 922–929.

5 A. S. Hoffman, *Adv. Drug Delivery Rev.*, 2013, **65**, 10–16.

6 H. Sun, C. P. Kabb, M. B. Sims and B. S. Sumerlin, *Prog. Polym. Sci.*, 2019, **89**, 61–75.

7 P. Yang, F. Zhu, Z. Zhang, Y. Cheng, Z. Wang and Y. Li, *Chem. Soc. Rev.*, 2021, **50**, 8319–8343.

8 Y. Hiruta, *Polym. J.*, 2022, **54**, 1419–1430.

9 D. Roy, W. L. A. Brooks and B. S. Sumerlin, *Chem. Soc. Rev.*, 2013, **42**, 7214.

10 F. Doberenz, K. Zeng, C. Willems, K. Zhang and T. Groth, *J. Mater. Chem. B*, 2020, **8**, 607–628.

11 Q. Zhang and R. Hoogenboom, *Prog. Polym. Sci.*, 2015, **48**, 122–142.

12 M. Sponchioni, U. C. Palmiero and D. Moscatelli, *Mater. Sci. Eng., C*, 2019, **102**, 589–605.

13 L. Sixdenier, A. Augé, Y. Zhao, E. Marie and C. Tribet, *ACS Macro Lett.*, 2022, **11**, 651–656.

14 A. Bordat, T. Boissenot, J. Nicolas and N. Tsapis, *Adv. Drug Delivery Rev.*, 2019, **138**, 167–192.

15 H. G. Schild and D. A. Tirrell, *J. Phys. Chem.*, 1990, **94**, 4352–4356.

16 J.-F. Lutz, K. Weichenhan, Ö. Akdemir and A. Hoth, *Macromolecules*, 2007, **40**, 2503–2508.

17 Y. Hiruta, Y. Nagumo, A. Miki, T. Okano and H. Kanazawa, *RSC Adv.*, 2015, **5**, 73217–73224.

18 D. E. Bergbreiter and H. Fu, *J. Polym. Sci., Part A: Polym. Chem.*, 2008, **46**, 186–193.

19 C. Porsch, S. Hansson, N. Nordgren and E. Malmström, *Polym. Chem.*, 2011, **2**, 1114–1123.

20 J.-F. Lutz, *J. Polym. Sci., Part A: Polym. Chem.*, 2008, **46**, 3459–3470.

21 S. Nishimura, K. Nishida, T. Ueda, S. Shiomoto and M. Tanaka, *Polym. Chem.*, 2022, **13**, 2519–2530.

22 A. A. A. Smith, C. L. Maikawa, H. L. Hernandez and E. A. Appel, *Polym. Chem.*, 2021, **12**, 1918–1923.

23 D. G. Lessard, M. Ousalem and X. X. Zhu, *Can. J. Chem.*, 2001, **79**, 1870–1874.

24 N. S. Ieong, M. Hasan, D. J. Phillips, Y. Saaka, R. K. O'Reilly and M. I. Gibson, *Polym. Chem.*, 2012, **3**, 794.

25 P. J. Roth, F. D. Jochum, F. R. Forst, R. Zentel and P. Theato, *Macromolecules*, 2010, **43**, 4638–4645.

26 A. Podevyn, K. Arys, V. R. de la Rosa, M. Glassner and R. Hoogenboom, *Eur. Polym. J.*, 2019, **120**, 109273.

27 Y. Hiruta, Y. Nagumo, Y. Suzuki, T. Funatsu, Y. Ishikawa and H. Kanazawa, *Colloids Surf., B*, 2015, **132**, 299–304.

28 Y. Zhang, S. Furyk, D. E. Bergbreiter and P. S. Cremer, *J. Am. Chem. Soc.*, 2005, **127**, 14505–14510.

29 R. Hoogenboom, H. M. L. Thijs, D. Wouters, S. Hoeppener and U. S. Schubert, *Soft Matter*, 2008, **4**, 103–107.

30 F. M. Winnik, H. Ringsdorf and J. Venzmer, *Macromolecules*, 1990, **23**, 2415–2416.

31 R. Hoogenboom, H. M. L. Thijs, M. J. H. C. Jochems, B. M. van Lankvelt, M. W. M. Fijten and U. S. Schubert, *Chem. Commun.*, 2008, 5758.

32 I. Akar, R. Keogh, L. D. Blackman, J. C. Foster, R. T. Mathers and R. K. O'Reilly, *ACS Macro Lett.*, 2020, **9**, 1149–1154.

33 I. Akar, J. C. Foster, X. Leng, A. K. Pearce, R. T. Mathers and R. K. O'Reilly, *ACS Macro Lett.*, 2022, **11**, 498–503.

34 G. H. Gu, J. Noh, I. Kim and Y. Jung, *J. Mater. Chem. A*, 2019, **7**, 17096–17117.

35 K. Rajan, *Annu. Rev. Mater. Res.*, 2015, **45**, 153–169.

36 R. Ramprasad, R. Batra, G. Pilania, A. Mannodi-Kanakkithodi and C. Kim, *npj Comput. Mater.*, 2017, **3**, 54.

37 Y. Oaki and Y. Igarashi, *Bull. Chem. Soc. Jpn.*, 2021, **94**, 2410–2422.

38 N. E. Jackson, M. A. Webb and J. J. de Pablo, *Curr. Opin. Chem. Eng.*, 2019, **23**, 106–114.

39 J. N. Kumar, Q. Li, K. Y. T. Tang, T. Buonassisi, A. L. Gonzalez-Oyarce and J. Ye, *npj Comput. Mater.*, 2019, **5**, 73.

40 H. Tokuyama, H. Mori, R. Hamaguchi and G. Kato, *Chem. Eng. Sci.*, 2021, **231**, 116325.

41 R. Tibshirani, M. Wainwright and T. Hastie, *Statistical Learning with Sparsity: The Lasso and Generalizations*, Chapman and Hall/CRC, Philadelphia, PA, 2015.

42 E. Candès and J. Romberg, *Inverse Probl.*, 2007, **23**, 969–985.

43 R. Mizuguchi, Y. Igarashi, H. Imai and Y. Oaki, *Nanoscale*, 2021, **13**, 3853–3859.

44 H. Numazawa, Y. Igarashi, K. Sato, H. Imai and Y. Oaki, *Adv. Theory Simul.*, 2019, **2**, 1900130.

45 K. Sakano, Y. Igarashi, H. Imai, S. Miyakawa, T. Saito, Y. Takayanagi, K. Nishiyama and Y. Oaki, *ACS Appl. Energy Mater.*, 2022, **5**, 2074–2082.

46 Y. Hiruta, R. Kanazashi, E. Ayano, T. Okano and H. Kanazawa, *Analyst*, 2016, **141**, 910–917.

47 T. Nishio, R. Kanazashi, A. Nojima, H. Kanazawa and T. Okano, *J. Chromatogr. A*, 2012, **1228**, 148–154.

48 G.-T. Chen, C.-H. Wang, J.-G. Zhang, Y. Wang, R. Zhang, F.-S. Du, N. Yan, Y. Kou and Z.-C. Li, *Macromolecules*, 2010, **43**, 9972–9981.

49 Y. Hiruta, M. Shimamura, M. Matsuura, Y. Maekawa, T. Funatsu, Y. Suzuki, E. Ayano, T. Okano and H. Kanazawa, *ACS Macro Lett.*, 2014, **3**, 281–285.

50 H. Mori, H. Iwaya, A. Nagai and T. Endo, *Chem. Commun.*, 2005, 4872.

51 T. Maeda, K. Yamamoto and T. Aoyagi, *J. Colloid Interface Sci.*, 2006, **302**, 467–474.

52 Y. Kametani, F. Tournilhac, M. Sawamoto and M. Ouchi, *Angew. Chem., Int. Ed.*, 2020, **59**, 5193–5201.

53 J.-F. Lutz, Ö. Akdemir and A. Hoth, *J. Am. Chem. Soc.*, 2006, **128**, 13046–13047.

54 H. Kanazawa, E. Ayano, C. Sakamoto, R. Yoda, A. Kikuchi and T. Okano, *J. Chromatogr. A*, 2006, **1106**, 152–158.